PHYSICAL REVIEW D **77,** 014010 (2008)

Isospin violation in ϕ, J/ψ, $\psi' \to \omega\pi^0$ via hadronic loops

Gang Li,[1] Qiang Zhao,[1,2] and Bing-Song Zou[1,3]

[1]*Institute of High Energy Physics, Chinese Academy of Sciences, Beijing 100049, People's Republic of China*
[2]*Department of Physics, University of Surrey, Guildford, GU2 7XH, United Kingdom*
[3]*CCAST, Beijing 100080, People's Republic of China*

(Received 4 June 2007; revised manuscript received 24 October 2007; published 11 January 2008)

In this work, we study the isospin-violating decay of $\phi \to \omega\pi^0$ and quantify the electromagnetic (EM) transitions and intermediate meson exchanges as two major sources of the decay mechanisms. In the EM decays, the present datum status allows a good constraint on the EM decay form factor in the vector meson dominance model, and it turns out that the EM transition can only account for about $1/4 \sim 1/3$ of the branching ratio for $\phi \to \omega\pi^0$. The intermediate meson exchanges, $K\bar{K}(K^*)$ (intermediate $K\bar{K}$ interaction via K^* exchanges), $K\bar{K}^*(K)$ (intermediate $K\bar{K}^*$ rescattering via kaon exchanges), and $K\bar{K}^*(K^*)$ (intermediate $K\bar{K}^*$ rescattering via K^* exchanges), which evade the naive Okubo-Zweig-Iizuka rule, serve as another important contribution to the isospin violations. They are evaluated with effective Lagrangians where explicit constraints from experiment can be applied. Combining these three contributions, we obtain results in good agreement with the experimental data. This approach is also extended to $J/\psi(\psi') \to \omega\pi^0$, where we find contributions from the $K\bar{K}(K^*)$, $K\bar{K}^*(K)$, and $K\bar{K}^*(K^*)$ loops are negligibly small, and the isospin violation is likely to be dominated by the EM transition.

DOI: 10.1103/PhysRevD.77.014010 PACS numbers: 13.25.−k, 12.40.Vv, 13.20.Gd

I. INTRODUCTION

The isospin breaking decay channel $\phi \to \omega\pi^0$ has been measured by experiment with improved precisions [1], and the Particle Data Group quote $\mathrm{BR}(\phi \to \omega\pi^0) = (5.2^{+1.3}_{-1.1}) \times 10^{-5}$ as the world average for its branching ratio [2]. This decay channel is very interesting due to the presence of the Okubo-Zweig-Iizuka (OZI) rule violation and isospin symmetry breaking together. These two mechanisms, which generally account for different aspects of the underlying dynamics, are correlated in this channel. With the availability of much improved experimental information about other related transitions, one can pursue a quantitative study of the underlying dynamics and learn more about the correlation between the OZI rule violation and isospin symmetry breaking in the nonperturbative regime.

The electromagnetic (EM) decay of $\phi \to \omega\pi^0$ is an important source of isospin violations, where the s and $\bar{s}$ annihilate into a virtual photon, which then decays into $\omega\pi^0$. The other source of isospin violation originates from the mass differences between the u and d quark [3]. It can contribute to $\phi \to \omega\pi^0$ via OZI-rule-violating strong decays.

In the literature the isospin violation in $\phi \to \omega\pi^0$ was studied by isoscalar and isovector mixing, e.g. $\phi - \omega - \rho^0$ and $\eta' - \eta - \pi^0$ mixings [4–9]. This scenario contains both EM and strong transitions in an s-channel, and allow the $\phi \to \omega\pi^0$ decay without violating the OZI rule [10]. In such an approach, the EM and strong decays cannot be separated out. An alternative view is to separate the EM and strong processes by explicitly introducing the EM amplitude as an s-channel process, and then including the hadronic loop contributions as the t-channel processes. This will be our focus in this work. Our strategy is to constrain the EM transition first, and a well-defined EM transition will then allow us to make a reliable evaluation of the strong isospin violation mechanism.

The EM transitions can be studied in the vector meson dominance (VMD) model. Recently, a systematic investigation of the role played by the EM transitions in $J/\psi(\psi') \to VP$, where V and P denote light nonet vector and pseudoscalar mesons, respectively, was reported in Refs. [11,12], and the up-to-date experimental data provided a good constraint on the VMD model. For $\phi \to \omega\pi^0$, the VMD approach has great advantages: on the one hand, the ϕ and ω meson masses are very close to the ρ mass. Hence, the EM form factors can be constrained by the precise data for the ρ^0 meson mass and width [2]. On the other hand, since other heavier vectors are rather far away from this kinematic region, their contributions to the form factor will be limited. The dominant mechanisms can thus be clarified. The availability of experimental information for $\phi \to \gamma\pi^0$ and $\rho\pi + \pi^+\pi^-\pi^0$ [13] is also an advantage for quantifying the EM contributions.

The isospin-violating strong decay can be related to the OZI rule violation at low energies via intermediate hadronic loops as proposed by Lipkin [14,15]. Microscopic interpretation of such a scenario as a mechanism for the OZI rule violation was investigated by Geiger and Isgur in a quark model [16,17]. For instance, an $s\bar{s}$ pair of 1^- can couple to nonstrange $n\bar{n} \equiv (u\bar{u} + d\bar{d})/\sqrt{2}$ via $K\bar{K}$, $K^*\bar{K}$ + c.c., etc. Suppressions of such an OZI-rule-violating process come from the cancellations between the intermediate meson loops and off-shell effects on the intermediate states [18,19]. Qualitatively, at high energies, where the mass scale of the intermediate states becomes unimportant, one would expect a ‘‘perfect cancellation’’ among all those intermediate states, and it recovers the OZI rule. At low energies, where the mass scale of the individual states is dominant, the perfect cancellation will break down due to e.g. $m_u \neq m_d$ originated from the chiral symmetry breaking. The OZI rule violations hence give rise to the recognition of isospin symmetry breakings.

Such a mechanism in $\phi \to \omega\pi^0$ decay can be described as follows: In $\phi \to \omega\pi^0$, the intermediate charged and neutral kaon loop transitions are supposed to cancel out if the isospin symmetry is conserved. However, due to small mass differences between the u and d quarks, the charged and neutral kaons will also have small differences in mass, i.e. $m_{K^0} - m_{K^\pm} = 3.972 \pm 0.027$ MeV [2], and they are coupled to the ϕ meson with slightly different strength. The hadronic loops will then have "imperfect" cancellations and lead to measurable isospin-violating branching ratios. This drives us to investigate the contributions from the intermediate meson exchanges to $\phi \to \omega\pi^0$, which is not only an OZI-rule-violating mechanism, but also a source of isospin violations.

A reasonable approach is that at hadronic level, we study the EM and hadronic loop contributions coherently with the aid of the up-to-date experimental data. It will enable us to quantify these two isospin-violating sources with some obvious advantages: (i) At hadronic level, we can extract couplings from independent experimental measurements without knowing all the details about the quark distribution functions. This technique has been broadly applied to the study of nonperturbative long-range interactions in the hadronic decays of heavy quarkonia, especially in charmonium decays [20–24]. (ii) Adopting the experimental constraints on the meson masses and effective couplings, we also avoid the details about how the difference of the $u - d$ quark masses leads to the corrections to the decay constants.

In the next section, we first analyze the EM ϕ decay in a VMD model and then present our intermediate-meson-exchange model with effective Lagrangians. The numerical results for $\phi \to \omega\pi^0$ are given in Sec. III. An extension of this approach to $J/\psi(\psi') \to \omega\pi^0$ is also discussed. A summary is then given in Sec. IV.

II. THE MODEL

A. Electromagnetic decay in VMD model

The $V\gamma^*$ coupling is described by the VMD model [25],

$$\mathcal{L}_{V\gamma} = \sum_V \frac{eM_V^2}{f_V} V_\mu A^\mu, \tag{1}$$

where eM_V^2/f_V is a direct photon-vector-meson coupling in Feynman diagram language, and the isospin 1 and 0 component of the EM field are both included. It should be noted that this form of interaction is only an approximation and can have large off-shell effects arising from either off-shell vector meson or virtual photon fields. In this approach we consider such effects in the $V\gamma P$ coupling form factor which will then be absorbed into the energy-dependent widths of the vector mesons.

The typical effective Lagrangian for the $V\gamma P$ coupling is

$$\mathcal{L}_{V\gamma P} = \frac{g_{V\gamma P}(q^2)}{M_V} \epsilon_{\mu\nu\alpha\beta} \partial^\mu V^\nu \partial^\alpha A^\beta P, \tag{2}$$

where $V^\nu (= \rho, \omega, \phi, J/\psi, \psi' \ldots)$ and A^β are the vector meson and EM field, respectively; M_V is the vector meson mass; $\epsilon_{\mu\nu\alpha\beta}$ is the antisymmetric Levi-Civita tensor. The coupling constant $g_{V\gamma P}(q^2)$ is off-shell and involves a form factor due to the virtuality of the photon. It can be expressed as

$$g_{V\gamma P}(q^2) = g_{V\gamma P}(0)\mathcal{F}(q^2), \tag{3}$$

where $g_{V\gamma P}(0)$ is the on-shell coupling and can be determined by vector meson radiative decays [11,12], e.g. $\omega \to \gamma\pi^0$ and $\phi \to \gamma\pi^0$.

In the VMD model, we can decompose the virtual photon by a sum of vector mesons as shown by Fig. 1. The amplitude for process-I [i.e. Fig. 1(I)] can be expressed as

$$M_{fi}^{\mathrm{EM-I}} = \sum_V \frac{e}{f_V} \frac{M_V^2}{M_\phi^2 - M_V^2 + iM_V\Gamma_V} \frac{e}{f_\phi} \times \frac{g_{\omega V\pi}}{M_\omega} \varepsilon_{\alpha\beta\mu\nu} p_\omega^\alpha \varepsilon_\omega^\beta p_\phi^\mu \varepsilon_\phi^\nu, \tag{4}$$

where $g_{\omega V\pi}$ is the VVP strong coupling constant, and Γ_V is the total width of the intermediate vector meson. This gives

$$g_{V\gamma P}(q^2) = g_{V\gamma P}(0)\mathcal{F}(q^2) = \sum_V g_{\omega V\pi} \frac{e}{f_V} \frac{M_V^2}{M_\phi^2 - M_V^2 + iM_V\Gamma_V}, \tag{5}$$

which relates the on-shell coupling $g_{V\gamma P}(0)$ to an off-shell coupling with form factors.

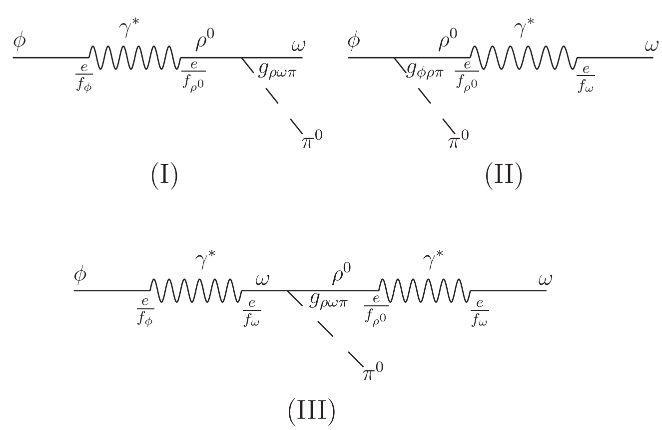

FIG. 1. Schematic diagrams for the EM transitions in $\phi \to \omega\pi^0$.

Similarly, the transition matrix element for process-II [Fig. 1(II)] can be written as

$$M_{fi}^{\mathrm{EM-II}} = \sum_V \frac{e}{f_V} \frac{M_V^2}{M_\omega^2 - M_V^2 + iM_V\Gamma_V} \frac{e}{f_\omega} \times \frac{g_{\phi V\pi}}{M_\phi} \varepsilon_{\alpha\beta\mu\nu} p_\omega^\alpha \varepsilon_\omega^\beta p_\phi^\mu \varepsilon_\phi^\nu, \quad (6)$$

where $g_{\phi V\pi}$ is again the strong coupling constant.

In the VMD framework, it also allows contributions from process-III [Fig. 1(III)] of which the expression is

$$M_{fi}^{\mathrm{EM-III}} = \sum_{V_1V_2} \frac{e}{f_{V_1}} \frac{e}{f_{V_2}} \frac{M_{V_1}^2}{M_\phi^2 - M_{V_1}^2 + iM_{V_1}\Gamma_{V_1}} \times \frac{M_{V_2}^2}{M_\omega^2 - M_{V_2}^2 + iM_{V_2}\Gamma_{V_2}} \frac{e}{f_\omega} \frac{e}{f_\phi} \times \frac{g_{V_1V_2\pi}}{M_{V_1}} \varepsilon_{\alpha\beta\mu\nu} p_\omega^\alpha \varepsilon_\omega^\beta p_\phi^\mu \varepsilon_\phi^\nu, \quad (7)$$

where V_1 and V_2 are intermediate vector mesons which are different from ω and ϕ when they are connected to these two states by the virtual photon. However, since we adopt experimental data for $\phi \to \rho^0\pi^0$ in process-II to determine the $g_{\phi\rho^0\pi^0}$ coupling, contributions from process-III will have been included in process-II. Nonetheless, we note in advance that exclusive contributions from process-III are negligibly small. Therefore, we will only concentrate on the first two processes in this study.

The following points can be made about $\phi \to \omega\pi^0$:

(i) We argue that the dominant contributions are from ρ^0 in this kinematics. Contributions from higher states will be relatively suppressed because their masses are larger than the virtuality of the photon. Other suppressions from the $V\gamma^*$ and VVP couplings are also expected. Basically, those higher vector mesons are farther away from the ϕ and ω masses than the ρ^0. We thus make an approximation of Eqs. (4) and (6) by considering only the ρ meson contributions:

$$M_{fi}^{\mathrm{EM}} = M_{fi}^{\mathrm{EM-I}} + M_{fi}^{\mathrm{EM-II}} \equiv \frac{\tilde{g}_{\mathrm{EM}}}{M_\phi} \varepsilon_{\alpha\beta\mu\nu} p_\omega^\alpha \varepsilon_\omega^\beta p_\phi^\mu \varepsilon_\phi^\nu, \quad (8)$$

where the EM coupling $\tilde{g}_{\mathrm{EM}}$ has a form

$$\tilde{g}_{\mathrm{EM}} \simeq \frac{e}{f_\rho}\left[\frac{e}{f_\phi}\left(\frac{M_\phi}{M_\omega}\right)\frac{M_\rho^2}{M_\phi^2 - M_\rho^2 + iM_\rho\Gamma_\rho} g_{\omega\rho^0\pi^0} + \frac{e}{f_\omega}\frac{M_\rho^2}{M_\omega^2 - M_\rho^2 + iM_\rho\Gamma_\rho} g_{\phi\rho^0\pi^0}\right], \quad (9)$$

with Γ_ρ and Γ_ω the total widths of ρ^0 and ω, respectively.

(ii) The vector-meson-photon couplings, e/f_V, can be determined by $V \to e^+e^-$:

$$\frac{e}{f_V} = \left[\frac{3\Gamma_{V\to e^+e^-}}{2\alpha_e|\mathbf{p}_e|}\right]^{1/2}, \quad (10)$$

where $|\mathbf{p}_e|$ is the electron three-momentum in the vector meson rest frame, and $\alpha_e = 1/137$ is the fine-structure constant.

(iii) The coupling, $g^2_{\omega\rho^0\pi^0} \simeq 85$, can be well determined by either $\omega \to \gamma\pi^0$ or $\omega \to \pi^0 e^+e^-$ [2] in the same framework.

(iv) For $g_{\phi\rho^0\pi^0}$, the KLOE measurement suggests that $\phi \to \rho\pi \to \pi^+\pi^-\pi^0$ has a weight of 0.937 in $\phi \to \pi^+\pi^-\pi^0$ [13]. This gives

$$0.937 \times \Gamma^{\mathrm{exp}}_{\phi\to\rho\pi+\pi^+\pi^-\pi^0} = \frac{|\mathbf{p}|^3}{12\pi M_\phi^2}(g_{\phi\rho^0\pi^0} + g_{\phi\rho^+\pi^-} + g_{\phi\rho^-\pi^+})^2, \quad (11)$$

with $|\mathbf{p}|$ denoting the three-vector momentum of the final state meson in the ϕ-rest frame. It is reasonable to assume $g_{\phi\rho^0\pi^0} = g_{\phi\rho^+\pi^-} = g_{\phi\rho^-\pi^+}$, Thus, the coupling constant can be determined: $g_{\phi\rho^0\pi^0} = 0.68$.

On the other hand, the coupling $g_{\phi\rho^0\pi^0}$ can be extracted in $\phi \to \gamma\pi^0$ by assuming that the ρ^0 is the dominant contribution to the form factor. This leads to

$$g_{\phi\rho^0\pi^0} = \left(\frac{12\pi M_\phi^2\Gamma_{\phi\to\gamma\pi^0}}{|\mathbf{p}|^3(e/f_\rho)^2}\frac{(M_\rho^2 + \Gamma_\rho^2)}{M_\rho^2}\right)^{1/2} \simeq 0.68, \quad (12)$$

where the ρ meson width is included. These two results are in excellent agreement with each other and highlight the necessity of considering the width effects of the ρ^0 pole in the form factor. Also, this evidently shows that the ρ^0 pole is the dominant contribution in the ϕ meson radiative decays, and the VMD approach indeed provides a reliable description of the EM transitions in $\phi \to \omega\pi^0$.

In the above treatment, all the couplings are determined by experimental data and there is no free parameter in the calculation of the EM decay couplings.

B. Intermediate $K\bar{K}(K^*)$ + c.c. loop

As discussed in the introduction, in principle, one should include all the possible intermediate-meson-exchange loops in the calculation. In reality, the breakdown of the local quark-hadron duality allows us to pick up the leading contributions as a reasonable approximation [14,15]. In the ϕ meson decay, the leading branching ratio is via $\phi \to K\bar{K}$, which makes the intermediate $K\bar{K}$ rescattering via K^* exchange a dominant contribution. Apart from this, $\phi K^*\bar{K}$ coupling is sizeable in the SU(3) flavor symmetry which also makes the intermediate $K\bar{K}^*$ + c.c. rescattering via kaon and/or K^* exchange important contributions in $\phi \to \omega\pi^0$. Contributions from higher mass states turn to be suppressed at the ϕ mass region. We take this as a reasonable approximation in this work, and formulate the contributions from (i) intermediate $K\bar{K}(K^*)$ loop; (ii) intermediate $K\bar{K}^*(K)$ loop; and (iii) intermediate $K\bar{K}^*(K^*)$ loop.

The transition amplitude for $\phi \to \omega\pi^0$ via an intermediate meson loop can be expressed as follows:

$$M_{fi} = \int \frac{d^4 p_2}{(2\pi)^4} \sum_{K^* \mathrm{pol}} \frac{T_1 T_2 T_3}{a_1 a_2 a_3} \mathcal{F}(p_2^2). \tag{13}$$

For $K\bar{K}(K^*)$, the vertex functions are

$$\begin{cases} T_1 \equiv i g_1 (p_1 - p_3) \cdot \varepsilon_\phi \\ T_2 \equiv \frac{i g_2}{M_\omega} \varepsilon_{\alpha\beta\mu\nu} p_\omega^\alpha \varepsilon_\omega^\beta p_2^\mu \varepsilon_2^\nu \\ T_3 \equiv i g_3 (p_\pi + p_3) \cdot \varepsilon_2, \end{cases} \tag{14}$$

where g_1, g_2, and g_3 are the coupling constants at the meson interaction vertices (see Fig. 1). The four vectors, p_ϕ, p_ω, and p_{π^0}, are the momenta for the initial ϕ and final state ω and π meson; the four-vector momentum, p_1, p_2, and p_3, are for the intermediate mesons, respectively; while $a_1 = p_1^2 - m_1^2$, $a_2 = p_2^2 - m_2^2$, and $a_3 = p_3^2 - m_3^2$ are the denominators of the propagators of intermediate mesons.

The form factor $\mathcal{F}(p^2)$, which takes care of the off-shell effects of the exchanged particles, is usually parameterized as

$$\mathcal{F}(p^2) = \left(\frac{\Lambda^2 - m^2}{\Lambda^2 - p^2}\right)^n, \tag{15}$$

where $n = 0, 1, 2$ correspond to different treatments of the loop integrals.

The coupling constants for the charged and neutral meson interactions are denoted by subscription "c" and "n," respectively. In the charged meson exchange loop, coupling g_{1c} can be determined by the experimental data for $\phi \to K^+K^-$ + c.c,

$$g_{1c}^2 = \frac{6\pi M_\phi^2}{|\mathbf{P}_{1c}|^3} \Gamma_{\phi \to K^+K^- + \mathrm{c.c.}}, \tag{16}$$

where $\Gamma_{\phi \to K^+K^- + \mathrm{c.c.}} = (49.2 \pm 0.6)\% \times \Gamma_{\mathrm{tot}}$ [2]. For the neutral channel, g_{1n} is determined by $\phi \to K^0\bar{K}^0$ + c.c. for which we adopt $\Gamma_{\phi \to K_S K_L} = (34.0 \pm 0.5)\% \times \Gamma_{\mathrm{tot}}$ [2] to derive

$$g_{1n}^2 = \frac{6\pi M_\phi^2}{|\mathbf{P}_{1n}|^3} \Gamma_{\phi \to K_S K_L}. \tag{17}$$

The coupling constant g_{3c} and g_{3n} can be deduced through the decay $K^* \to K\pi$. For example, g_{3n} is determined by $K^{*0} \to K^0\pi^0$:

$$g_{3n}^2 = g_{K^{*0}K^0\pi^0}^2 = \frac{6\pi M_{K^{*0}}^2}{|\mathbf{P}|^3} \Gamma_{K^{*0} \to K^0\pi^0}. \tag{18}$$

It shows that within the precision of the experimental data for $K^{*0} \to K^0\pi^0$ and $K^{*\pm} \to K^\pm\pi^\mp$, coupling $g_{K^{*0}K^0\pi^0}$ has the same value as $g_{K^{*\pm}K^\pm\pi^\mp}$. The extracted values are listed in Table I.

The relative signs between the couplings are determined by the SU(3) flavor symmetry relations [26]:

$$g_{3c} = -g_{3n} = g_{K^{*-}K^-\pi^0} = -g_{K^{*+}K^+\pi^0} = g_{K^{*0}K^0\pi^0} = -g_{\bar{K}^{*0}\bar{K}^0\pi^0}. \tag{19}$$

Note that the above equation is to illustrate the relative signs instead of the values for the coupling constants.

The coupling constant g_2 cannot be directly derived from experiment. But it can be related to the $\omega\rho^0\pi^0$ coupling via the SU(3) flavor symmetry:

$$g_{2c} = g_{2n} = g_{\omega K^{*-}K^+} = g_{\omega K^{*+}K^-} = g_{\omega \bar{K}K^0} = g_{\omega K^{*0}\bar{K}^0} = g_{\omega\rho^0\pi^0}/2, \tag{20}$$

where, again, the relative signs between the charged and neutral couplings are determined by Ref. [26].

With the couplings determined as the above, one can see that a relative sign arises between the amplitudes for the charged and neutral meson exchange loops. We then distinguish these two amplitudes as follows:

$$M_{fi} \equiv M_{fi}^c + M_{fi}^n, \tag{21}$$

where M_{fi}^c and M_{fi}^n have similar structures except that the couplings and masses involving the intermediate charged and neutral mesons are different due to the isospin symmetry violations. The nonvanishing cancellation thus can contribute to the isospin-violating branching ratios.

To proceed, we treat the loop integral in two different ways. First, we apply an on-shell approximation (Cutkosky rule) for the intermediate $K\bar{K}$, which will reduce the loop integration into an integral over the azimuthal angles defined by $\mathbf{p}_3$ relative to $\mathbf{p}_\pi$. This approximation picks up the imaginary part of the transition amplitude, and with $n = 0$, 1, 2, we can examine the effects from the form factors. There are some disadvantages of this treatment. For intermediate mesons of which the mass threshold is above the ϕ mass, their contributions to the imaginary (absorptive) part vanish though their contributions to the real (dispersive) part may be sizeable. Because of this, we also consider the loop integrals including the dispersive part in a Feynman

TABLE I. The absolute values of coupling constants for the vertex interactions. Their relative phases are determined by the SU(3) flavor symmetry.

Coupling constants	$\lvert g_{\phi K\bar{K}}\rvert$	$\lvert g_{\omega K^*\bar{K}}\rvert$	$\lvert g_{K^*K\pi}\rvert(\lvert f_{K^*K\pi}\rvert)$	$\lvert f_{\phi K^*\bar{K}}\rvert$
Charged kaon coupling	4.49	4.58	3.96	6.48
Neutral kaon coupling	4.62	4.58	3.96	6.48

integration. To kill the ultraviolet divergences, we include the form factors with $n = 1$ and 2 for a monopole and dipole, respectively. Below are the details.

1. Integrations with on-shell approximation

By applying the Cutkosky rule to the loop integration, we can reduce the transition amplitude (e.g. for the charged meson loop) to be

$$M_{fi}^{c} = \frac{|\mathbf{p}_{3c}|}{32\pi^2 M_\phi}\int d\Omega \frac{T_c \mathcal{F}(P_{2c}^2)}{p_{2c}^2 - m_{2c}^2}, \tag{22}$$

with

$$T_c \equiv (T_1T_2T_3)_c = \frac{ig_{1c}g_{2c}g_{3c}}{M_\omega} 4\varepsilon_{\alpha\beta\mu\nu}\varepsilon_\omega^\alpha p_{3c}^\beta p_\pi^\mu p_\omega^\nu \varepsilon_\phi \cdot p_{3c}. \tag{23}$$

The integration is over the azimuthal angles of the momentum $\mathbf{p}_{3c}$ relative to the momentum of the final state π meson. The kinematics are defined as $p_\omega = (E_\omega, 0, 0, |\mathbf{P}_\omega|)$, $p_\pi = (E_\pi, 0, 0, -|\mathbf{P}_\omega|)$, and $p_{2c}^2 = (p_{3c} - p_\pi)^2 = M_\pi^2 + m_{3c}^2 - 2E_\pi E_{3c} + 2|\mathbf{P}_\pi||\mathbf{p}_{3c}|\cos\theta$.

Similarly, we obtain the amplitude for the neutral meson loop:

$$M_{fi}^{n} = \frac{|\mathbf{p}_{3n}|}{32\pi^2 M_\phi}\int d\Omega \frac{T_n \mathcal{F}(p_{2n}^2)}{p_{2n}^2 - m_{2n}^2}, \tag{24}$$

with

$$T_n \equiv (T_1T_2T_3)_n = \frac{ig_{1n}g_{2n}g_{3n}}{M_\omega} 4\varepsilon_{\alpha\beta\mu\nu}\varepsilon_\omega^\alpha p_{3n}^\beta p_\pi^\mu p_\omega^\nu \varepsilon_\phi \cdot p_{3n}. \tag{25}$$

Note that the momenta and masses for the intermediate states are different between the charged and neutral cases as denoted by the subscription "c" and "n," respectively.

The nonvanishing amplitudes require the vector meson polarizations to be taken as either $(\varepsilon_\omega, \varepsilon_\phi) = (+,-)$ or $(-,+)$. We then obtain

$$M_{fi}(+,-) = -M_{fi}(-,+) = -\frac{g_1g_2g_3|\mathbf{p}_3|^3|\mathbf{P}_\omega|}{8\pi M_\omega}\mathcal{I}, \tag{26}$$

where

$$\mathcal{I} \equiv \int \frac{\sin^2\theta \mathcal{F}(P_2^2)}{p_2^2 - m_2^2}\sin\theta d\theta. \tag{27}$$

(i) With no form factor, i.e., $\mathcal{F}(p_2^2) = 1$, the integral becomes

$$\mathcal{I} = \frac{1}{A_s}\left[\frac{2}{A^2} + \frac{A^2-1}{A^3}\log\frac{1+A}{1-A}\right]. \tag{28}$$

(ii) With a monopole form factor, i.e., $\mathcal{F}(p_2^2) = (\Lambda^2 - m_2^2)/(\Lambda^2 - p_2^2)$, the integral becomes

$$\mathcal{I} = \frac{m_2^2 - \Lambda^2}{A_sB_s}\left[-\frac{2}{AB} + \frac{A^2-1}{A^2(A-B)}\log\frac{1+A}{1-A} + \frac{1-B^2}{B^2(A-B)}\log\frac{1+B}{1-B}\right]. \tag{29}$$

(iii) With a dipole form factor, i.e., $\mathcal{F}(p_2^2) = [(\Lambda^2 - m_2^2)/(\Lambda^2 - p_2^2)]^2$, the integral becomes

$$\mathcal{I} = \frac{(m_2^2 - \Lambda^2)^2}{A_sB_s^2(A-B)^2}\left[-\frac{2B(A-B)(B^2-1)}{B^2(1-B^2)} + \frac{A^2-1}{A}\log\frac{1+A}{1-A} - \frac{AB^2 - 2B + A}{B^2}\log\frac{1+B}{1-B}\right]. \tag{30}$$

The kinematic functions are defined as

$$A_s = M_\omega^2 + m_1^2 - 2E_1E_\omega - m_2^2, \quad B_s = M_\omega^2 + m_1^2 - 2E_1E_\omega - \Lambda^2, \tag{31}$$

$$A = -2|\mathbf{p}_1||\mathbf{P}_\omega|/A_s, \qquad B = -2|\mathbf{p}_1||\mathbf{P}_\omega|/B_s. \tag{32}$$

2. Feynman integrations with form factors

With the form factors, the ultraviolet divergence in the Feynman integration can be avoided. For the charged meson loop as an example, the integral has an expression

$$\mathcal{M}_{fi}^{c} = \int \frac{d^4p_{2c}}{(2\pi)^4}\sum_{K^*\mathrm{pol}} \frac{[ig_{1c}(p_{1c} - p_{3c})\cdot\varepsilon_\phi][\frac{ig_{2c}}{M_\omega}\varepsilon_{\alpha\beta\mu\nu}p_\omega^\alpha\varepsilon_\omega^\beta p_{2c}^\mu\varepsilon_2^\nu][ig_{3c}(p_\pi + p_{3c})\cdot\varepsilon_2]}{(p_{1c}^2 - m_{1c}^2)(p_{3c}^2 - m_{3c}^2)(p_{2c}^2 - m_{2c}^2)}\mathcal{F}(p_{2c}^2). \tag{33}$$

With a monopole form factor, we have

$$\mathcal{M}_{fi}^{c} = -\frac{g_{1c}g_{2c}g_{3c}}{M_\omega}\varepsilon_{\alpha\beta\mu\nu}p_\omega^\alpha\varepsilon_\omega^\beta p_\phi^\mu\varepsilon_\phi^\nu \int_0^1 dx\int_0^{1-x} dy \frac{2}{(4\pi)^2}\log\frac{\triangle(m_{1c}, m_{3c}, \Lambda)}{\triangle(m_{1c}, m_{3c}, m_{2c})}, \tag{34}$$

while with a dipole form factor, we have

$$\mathcal{M}^c_{fi} = -\frac{g_{1c}g_{2c}g_{3c}}{M_\omega}\varepsilon_{\alpha\beta\mu\nu}p^\alpha_\omega\varepsilon^\beta_\omega p^\mu_\phi\varepsilon^\nu_\phi\int_0^1 dx \times\int_0^{1-x} dy\frac{2}{(4\pi)^2}\bigg[\log\frac{\triangle(m_{1c},m_{3c},\Lambda)}{\triangle(m_{1c},m_{3c},m_{2c})} \quad (35)$$

$$-\frac{y(\Lambda^2-m^2_{2c})}{\triangle(m_{1c},m_{3c},\Lambda)}\bigg], \quad (36)$$

where the function Δ is defined as

$$\Delta(a,b,c) \equiv M^2_\omega(1-x-y)^2 - (M^2_\phi - M^2_\omega - M^2_\pi)\times(1-x-y)x + M^2_\pi x^2 - (M^2_\omega - a^2)\times(1-x-y) - (M^2_\pi - b^2)x + yc^2. \quad (37)$$

Expressions for M^n_{fi} are essentially the same as M^c_{fi} with $g_{1c,2c,3c}$ and $m_{1c,2c,3c}$ replaced by $g_{1n,2n,3n}$ and $m_{1n,2n,3n}$, and we do not repeat them here in order to save space.

C. Intermediate $K\bar{K}^*(K)$ + c.c. loop

As shown by Fig. 2, the vertex functions for the $K\bar{K}^*(K)$ + c.c. loop are

$$\begin{cases} T_1 \equiv \frac{if_1}{M_\phi}\varepsilon_{\alpha\beta\mu\nu}p^\alpha_\phi\varepsilon^\beta_\phi p^\mu_3\varepsilon^\nu_3, \\ T_2 \equiv if_2(p_1-p_2)\cdot\varepsilon_\omega, \\ T_3 \equiv if_3(p_\pi-p_2)\cdot\varepsilon_3, \end{cases} \quad (38)$$

where $f_{1,2,3}$ are the coupling constants and $\mathcal{F}(p^2_2)$ is the form factor.

Similar to the previous section, one finds that a relative sign arises from the charged and neutral meson exchange loops, which can be distinguished by $M_{fi} \equiv M^c_{fi} + M^n_{fi}$. Thus, we have the expression for the charged amplitude with a monopole form factor

$$\mathcal{M}^c_{fi} = \frac{f_{1c}f_{2c}f_{3c}}{M_\omega}\varepsilon_{\alpha\beta\mu\nu}p^\alpha_\omega\varepsilon^\beta_\omega p^\mu_\phi\varepsilon^\nu_\phi\int_0^1 dx\int_0^{1-x}dy\frac{2}{(4\pi)^2}\times\log\frac{\triangle(m_{1c},m_{3c},\Lambda)}{\triangle(m_{1c},m_{3c},m_{2c})}, \quad (39)$$

and with a dipole form factor

$$\mathcal{M}^c_{fi} = \frac{f_{1c}f_{2c}f_{3c}}{M_\omega}\varepsilon_{\alpha\beta\mu\nu}p^\alpha_\omega\varepsilon^\beta_\omega p^\mu_\phi\varepsilon^\nu_\phi\int_0^1 dx \times\int_0^{1-x} dy\frac{2}{(4\pi)^2}\bigg[\log\frac{\triangle(m_{1c},m_{3c},\Lambda)}{\triangle(m_{1c},m_{3c},m_{2c})} \quad (40)$$

$$-\frac{y(\Lambda^2-m^2_{2c})}{\triangle(m_{1c},m_{3c},\Lambda)}\bigg]. \quad (41)$$

In the above two equations the intermediate meson masses $m_{1,2,3}$ are from the $K\bar{K}^*(K)$ loops, which are different from those in Eqs. (33) and (35).

In the $K\bar{K}^*(K)$ loop, the coupling constant $g_{\phi K^*K}$ is related to $g_{\omega\rho^0\pi^0}$ in the SU(3) flavor symmetry:

$$f_{1c} = f_{1n} = g_{\phi K^{*+}K^-} = g_{\phi K^{*-}K^+} = g_{\phi K^{*0}\bar{K}^0} = g_{\phi\bar{K}^{*0}K^0} = g_{\omega\rho^0\pi^0}/\sqrt{2}, \quad (42)$$

where we neglect the possible differences caused by the isospin violation between the charged and neutral channel. The reason is because these loop contributions are negligibly small and such a difference cannot produce measurable effects. At the $\omega K\bar{K}$ vertex, the coupling $g_{\omega K\bar{K}}$ can be related to $\phi K\bar{K}$ by the following relation:

$$\begin{aligned} f_{2c} &= g_{\omega K^+K^-} = -g_{\omega K^-K^+} = g_{\phi K^+K^-}/\sqrt{2}, \\ f_{2n} &= g_{\omega K^0\bar{K}^0} = -g_{\omega\bar{K}^0K^0} = g_{\phi K^0\bar{K}^0}/\sqrt{2}, \end{aligned} \quad (43)$$

where we assume that the isospin breaking in the $\omega K\bar{K}$ couplings is similar to that in the $\phi K\bar{K}$ ones.

The absolute values of the coupling constants are listed in Table I.

D. Intermediate $K\bar{K}^*(K^*)$ + c.c. loop

We also consider the transition amplitude from the intermediate $K\bar{K}^*(K^*)$ + c.c. loop (Fig. 2), which can be expressed the same form as Eq. (13) except that the vertex functions change to

$$\begin{cases} T_1 \equiv \frac{ih_1}{M_\phi}\varepsilon_{\alpha\beta\mu\nu}P^\alpha_\phi\varepsilon^\beta_\phi p^\mu_3\varepsilon^\nu_3, \\ T_2 \equiv \frac{ih_2}{m_2}\varepsilon_{\alpha'\beta'\mu'\nu'}p^{\alpha'}_2\varepsilon^{\beta'}_2 P^{\mu'}_\omega\varepsilon^{\nu'}_\omega, \\ T_3 \equiv \frac{ih_3}{m_3}\varepsilon_{\alpha''\beta''\mu''\nu''}p^{\alpha''}_2\varepsilon^{\beta''}_2 p^{\mu''}_3\varepsilon^{\nu''}_3, \end{cases} \quad (44)$$

where $h_{1,2,3}$ are the coupling constants and $\mathcal{F}(p^2_2)$ is the form factor.

Similar to the above sections, a relative sign arises from the charged and neutral meson exchange loops, i.e. $M_{fi} \equiv M^c_{fi} + M^n_{fi}$, and we only give here the expressions for the charged amplitude with a monopole and dipole form factor, respectively,

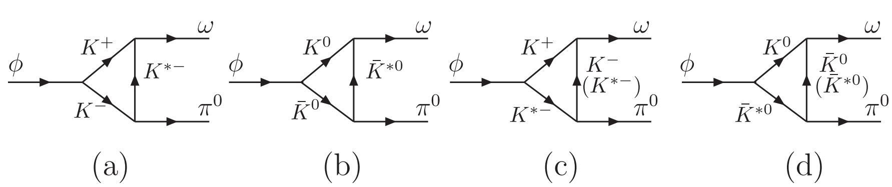

FIG. 2. Schematic picture for the decay of $\phi \to \omega\pi^0$ via $K\bar{K}(K^*)$, $K\bar{K}^*(K)$, and $K\bar{K}^*(K^*)$ intermediate meson loops.

$$M^c_{fi} = \frac{h_{1c}h_{2c}h_{3c}}{M_\phi m_{2c}m_{3c}} \epsilon_{\alpha\beta\mu\nu} p^\alpha_\omega \epsilon^\beta_\omega p^\mu_\phi \epsilon^\nu_\phi \int_0^1 dx \int_0^{1-x} dy \times \int_0^{1-x-y} dz \frac{2}{(4\pi)^2}\left[\frac{A}{\triangle_1} - \frac{B}{2\triangle_1^2}\right], \quad (45)$$

and

$$M^c_{fi} = -\frac{h_{1c}h_{2c}h_{3c}}{M_\phi m_{2c}m_{3c}} \epsilon_{\alpha\beta\mu\nu} p^\alpha_\omega \epsilon^\beta_\omega p^\mu_\phi \epsilon^\nu_\phi \int_0^1 dx \int_0^{1-x} dy \times \int_0^{1-x-y} dz \frac{2}{(4\pi)^2}\left[\frac{A}{\triangle_1^2} - \frac{B}{\triangle_1^3}\right], \quad (46)$$

with

$$A = \tfrac{1}{4}(2x + \tfrac{3}{2}z - 1)(M^2_\phi - M^2_\omega - M^2_{\pi^0}) + \tfrac{1}{2}xM^2_{\pi^0} + \tfrac{1}{4}zM^2_\omega,$$
$$B = (x + z - 1)xz[M^2_\omega M^2_{\pi^0} - \tfrac{1}{4}(M^2_\phi - M^2_\omega - M^2_{\pi^0})^2],$$
$$\triangle_1 = x^2M^2_{\pi^0} + z^2M^2_\omega - xz(M^2_\phi - M^2_\omega - M^2_{\pi^0}) - z(M^2_\omega - M^2_{1c}) + yM^2_{2c} - x(M^2_{\pi^0} - M^2_{3c}) + (1 - x - y - z)\Lambda^2. \quad (47)$$

In this transition loop the intermediate meson masses $m_{1,2,3}$ correspond to K, $\bar{K}^*$, and k^*. Quantities $h_{1,2,3}$ denote the corresponding vertex coupling constants with the relative signs given by

$$h_{3c} = -h_{3n} = -g_{\bar{K}^{*0}\bar{K}^{*0}\pi^0} = -g_{K^{*0}K^{*0}\pi^0} = -g_{K^{*+}K^{*+}\pi^0} = -g_{K^{*-}K^{*-}\pi^0} = g_{\omega\rho^0\pi^0}/2. \quad (48)$$

III. NUMERICAL RESULTS

A. Branching ratios from EM decay transition

The ϕ meson EM decay turns out to be very sensitive to the ρ^0 mass pole and decay width in the VMD model. This is because their masses are close to each other. As a test, in the infinitely narrow-width limit, i.e. $\Gamma_\rho = \Gamma_\omega = 0$ GeV, the branching ratio turns out to be overestimated: $\mathrm{BR}^{\mathrm{EM}} = 1.46 \times 10^{-4}$, which is more than 2 times the experimental value. This may not be surprising since one should adopt the mass eigenstates in the calculation instead of the isospin eigenstates in degenerate perturbation theory. Therefore, we apply the experimental data for the intermediate vector meson masses and widths in the calculation.

With the width of the ρ meson included, we obtain $\mathrm{BR}^{\mathrm{EM}} = 1.68 \times 10^{-5}$, with $M_\rho = 775.9$ MeV and $\Gamma_\rho = 143.9$ MeV [13]. With the PDG average, i.e. $M_\rho = 775.5$ MeV and $\Gamma_\rho = 149.4$ MeV, we have $\mathrm{BR}^{\mathrm{EM}} = 1.67 \times 10^{-5}$. This explicitly shows an important role played by the ρ meson.

We also examine the relative strength between process-I and II. Their exclusive contributions to the branching ratios are $\mathrm{BR}^{\mathrm{EM-I}} = 1.45 \times 10^{-5}$ and $\mathrm{BR}^{\mathrm{EM-II}} = 4.56 \times 10^{-7}$, respectively, which shows that process-I is dominant over II in the ϕ decay.

The above results suggest that the EM transition alone cannot account for the observed branching ratio for $\phi \to \omega\pi^0$. We hence need to look at the contributions from the intermediate meson exchanges.

B. Branching ratios from hadronic loop under on-shell approximation

Under the on-shell approximation only the intermediate $K\bar{K}$ will contribute since the threshold of any other strange meson pairs will be above the ϕ mass.

Without the form factor, the branching ratio from the $K\bar{K}(K^*)$ loop is 3.02×10^{-6}. This number is much smaller than the EM contributions. Apart from the significant cancellations between the charged and neutral channel amplitudes, another reason is because of the kinematic suppression on the absorptive amplitudes, i.e. the intermediate $K\bar{K}$ is close to the ϕ mass. Similar phenomena are observed in $J/\psi \to \gamma f_0(1810) \to \gamma\omega\phi$ at the higher mass tail of the $f_0(1810)$ [27]. At least it is reasonable to understand that contributions from near-threshold intermediate meson rescattering are limited in the on-shell approximation.

In order to investigate the role played by the form factors, we present the calculation results in Fig. 3 for three cases: (i) the hadronic loop has a dipole form factor (solid curve); (ii) the hadronic loop has a monopole form factor (dashed curve); and (iii) no form factors are included (dotted-dashed line). It is easy to understand that under the on-shell approximation the calculation without the form factors for the hadronic loops will have the largest contributions to the branching ratio. In contrast, the inclusion of

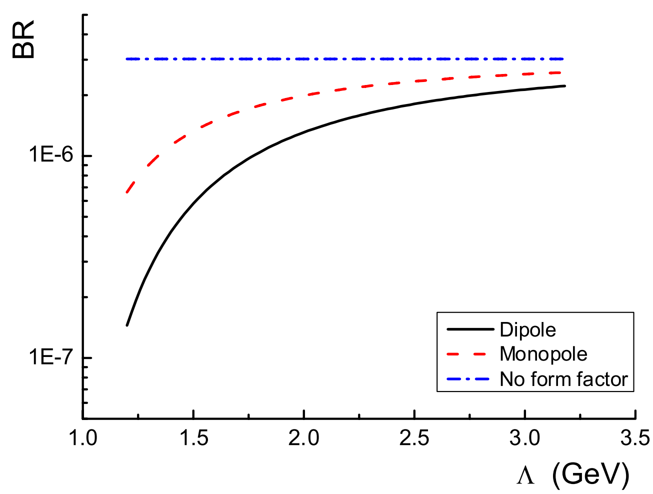

FIG. 3 (color online). The Λ dependence of the $K\bar{K}(K^*)$ loop contributions in the on-shell approximation. The dotted-dashed, dashed, and solid curve denote different considerations for the form factors, i.e. no form factor, monopole and dipole, respectively.

a monopole form factor suppresses the hadronic loop contributions, and a dipole form factor leads to the most suppressions. These three results then converge to the same value when $\Lambda \to \infty$ as shown in Fig. 3.

The overall results in terms of Λ including the EM and hadronic loop amplitudes are presented in Fig. 4 for two different phases, i.e. on the left panel the EM amplitude is out of phase to the hadronic loop (destructive addition), while on the right panel these two amplitudes are in phase (constructive addition). On the left panel the horizontal line reflects the largest cancellation between the EM and hadronic loop amplitudes with no form factor suppressions. At the small Λ region, the cancellations are small for both monopole and dipole calculations since the hadronic loop amplitudes are small in both cases as shown by Fig. 3. These three curves smoothly approach the same value at high Λ where the hadronic loop contributions become negligibly small.

On the right panel, the EM amplitude is in phase to the hadronic loop. In the case that no form factor is introduced in the hadronic loop, the constructive addition of the EM and hadronic loop amplitudes gives $\mathrm{BR} = 2.55 \times 10^{-5}$. For the monopole and dipole form factor, the constructive effects increase with parameter Λ since the exclusive hadronic loop contributions are small in the small Λ region. It shows by the dashed and solid curve that the inclusive branching ratios converge to the dotted-dashed curve at large Λ. In this constructive addition, the maximum branching ratio is still smaller than the experimental data, which is a sign for the underestimate of the hadronic loop contributions in the on-shell approximation, and implies the need for contributions from the dispersive part, i.e. from intermediate mesons above the ϕ mass.

C. Branching ratios from Feynman integrations

Note that we are interested in a small effect arising from cancellations between two sizeable amplitudes. Since the charged and neutral amplitudes distinguish themselves by the mass differences between the charged and neutral particles involved in the loop transition, it makes the behavior of the cancellations very sensitive to the choice of the cutoff energies. Again, it is necessary to investigate the Λ dependence of the hadronic loop integrals. We first study the exclusive behaviors of the $K\bar{K}(K^*)$, $K\bar{K}^*(K)$, and $K\bar{K}^*(K^*)$ loops and then combine them with the EM transitions to study their interferences.

In Fig. 5, the $K\bar{K}(K^*)$ loop in terms of the cutoff energy Λ is illustrated. The left panel is for a monopole form factor, while the right one is for a dipole type. The dashed and dotted-dashed curves are contributions from the charged and neutral meson loop, respectively, and the solid curves are their differences. In fact, the differences between the dashed and dotted-dashed curves are so small that it is hard to distinguish them as shown by the figures. Their cancellations leave only a small residue quantity accounting for the isospin violation effects.

The dependence of the details of the cancellations to the cutoff energy turns out to be more dramatic with a dipole form factor as shown by the right panel of Fig. 5. Although the integral for both the charged and neutral meson loops has a well-defined behavior, details of the cancellations as shown by the solid curve has an oscillatory behavior at small Λ. This is understandable since the difference between the charged and neutral meson loop integrals has a complicated dependence on the couplings, and the mass differences between the charged and neutral kaon and K^* in the propagators. For large Λ, the integral difference smooths out since Λ becomes the major energy scale.

In Fig. 5 there are dips appearing at small Λ for both monopole and dipole form factors. This is due to the factor $\Lambda^2 - m_{K^*}^2$ in the numerators of the form factors and the largest cancellation between the charged and neutral meson loops.

For the P-wave $\phi \to \omega\pi^0$ decay, the form factor favors a dipole behavior with relatively large Λ in order to account for the off-shell effects. Guided by the solid curve on the right panel of Fig. 5, we argue that $\Lambda \simeq 1.5 \sim 2$ GeV is appropriate for the hadronic loop contributions. Also, in this region, the integral difference has a well-defined smooth behavior. In the case of the monopole form factor, to describe the experimental data, Λ must have a relatively

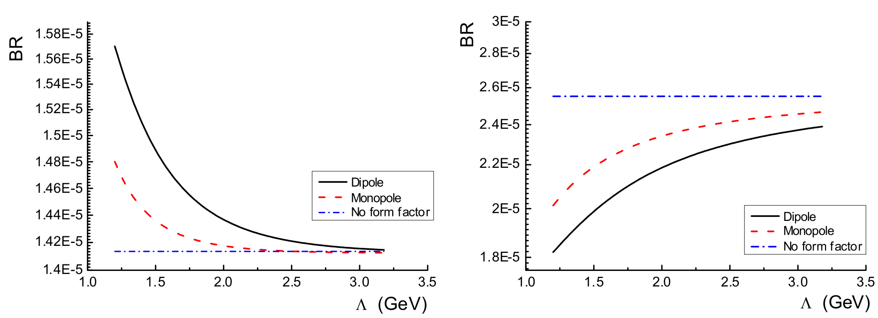

FIG. 4 (color online). The Λ dependence of the sum of the EM and $K\bar{K}(K^*)$ loop amplitudes in the on-shell approximation. The left panel indicates results for a destructive addition and the right panel for a constructive addition. The solid, dashed, and dotted-dashed curves denote different considerations for the form factors, i.e. dipole, monopole and no form factor, respectively.

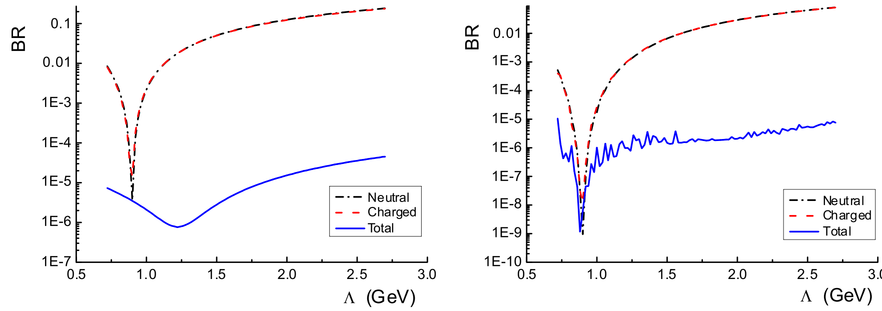

FIG. 5 (color online). The Λ dependence of the $K\bar{K}(K^*)$ loop contributions to the branching ratio in the Feynman integration. The left panel indicates results with a monopole form factor, and the right one with a dipole form factor. The dashed and dotted-dashed curves are contributions from only charged and neutral meson loop, respectively, while the solid curves are the results after cancellations between the charged and neutral amplitudes. We note that the dashed and dotted-dashed curves are close to each other and difficult to distinguish them by sight.

smaller value, i.e. <2 GeV. Otherwise, the branching ratio will be overestimated. Because of this ambiguity, we leave the value of Λ to be determined by the experimental data.

The $K\bar{K}^*(K)$ loop contributions are presented by Fig. 6 for the monopole and dipole form factors. Similar to Fig. 5, the intermediate charged and neutral meson loop contributions to the branching ratios are compared with each other as denoted by the dashed and dotted-dashed curves, while the solid curves are given by their amplitude differences. Interestingly, the $K\bar{K}^*(K)$ loop contributions turn out to exhibit a smooth behavior with both monopole and dipole form factors, and their magnitudes are comparable with the $K\bar{K}(K^*)$ loop. Again, the dips are related to the factor $\Lambda^2 - m_K^2$ in the numerator of the form factors and the largest cancellation between the charged and neutral meson loops.

In Fig. 7, the Λ dependence of the exclusive contributions from the $K\bar{K}^*(K^*)$ loop are presented. Compared with the other two loops, the exclusive branching ratio decreases in terms of the increasing Λ. As a result, its interferences with other channels around $\Lambda = 1.5 \sim 2.0$ GeV turn to be small.

Adding the hadronic loops to the EM amplitude coherently, we examine two phases in Fig. 8 in terms of the Λ, i.e. constructive (left panel) and destructive additions (right panel). It shows that with $\Lambda = 1.8 \sim 2.3$ GeV, the constructive addition with the dipole form factor for the hadronic loops gives the branching ratio in agreement with the experimental data, while with the monopole form factor, Λ requires a range of $1.2 \sim 1.5$ GeV. These cutoff energy ranges are consistent with the commonly accepted values. For a destructive addition between the EM and hadronic loop amplitudes as shown on the right panel, we find that the dipole form factor cannot reproduce the data within $\Lambda = 1 \sim 2.6$ GeV due to the significant cancellations between the EM and hadronic loop transitions. In contrast, with a monopole form factor for the hadronic loops the destructive addition can still reproduce the data around $\Lambda = 2.3$ GeV. However, this value of Λ turns out to be out of the commonly accepted range for a monopole cutoff energy. In this sense, it shows that the data favor a constructive phase between the EM and hadronic loop amplitudes.

The dipole form factor might be even more preferable. As we have discussed earlier that the P-wave decay will generally favor a dipole form factor, we hence argue that the constructive addition between the EM and hadronic loop amplitudes with a dipole form factor is a favorable mechanism accounting for the experimental observation of $\mathrm{BR}(\phi \to \omega\pi^0) = (5.2^{+1.3}_{-1.1}) \times 10^{-5}$ [2]. In Table II, branching ratios of the exclusive and coherent (construc-

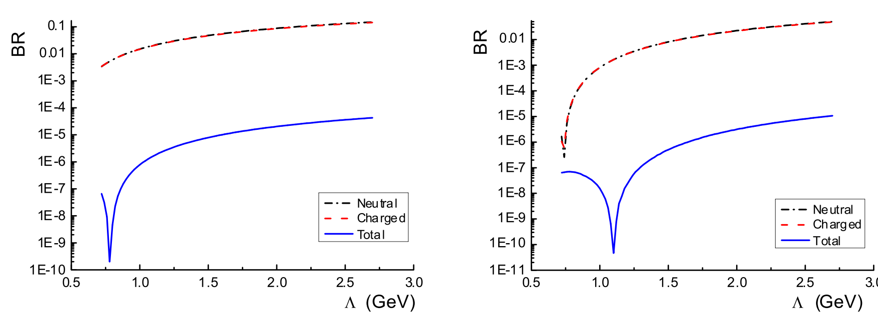

FIG. 6 (color online). The Λ dependence of the $K\bar{K}^*(K)$ loop contributions to the branching ratio in the Feynman integration. The notations are similar to Fig. 5. Again, we note that the dashed and dotted-dashed curves are difficult to distinguish by sight.

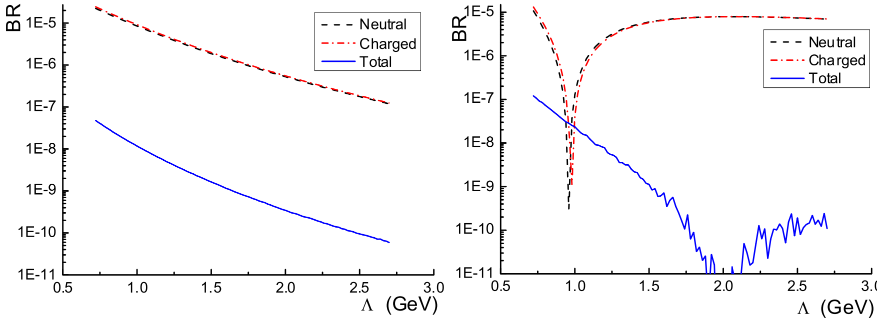

FIG. 7 (color online). The Λ dependence of the $K\bar{K}^*(K^*)$ loop contributions to the branching ratio in the Feynman integration. The notations are similar to Fig. 5. Again, we note that the dashed and dotted-dashed curves are difficult to distinguish by sight.

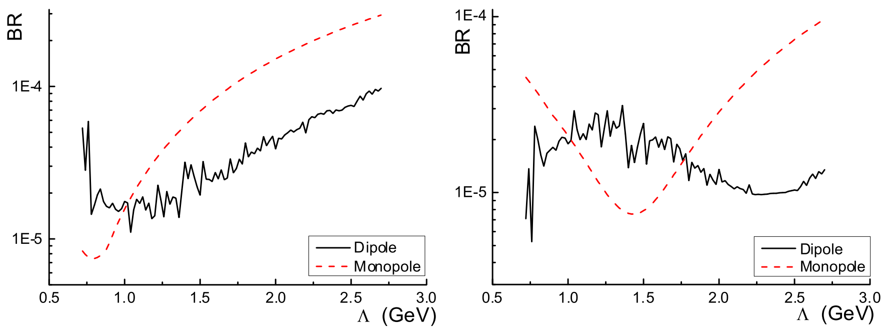

FIG. 8 (color online). The Λ dependence of the constructive (left panel) and destructive additions (right panel) between the EM and hadronic loops. The dashed curves denote the results for adopting a monopole form factor for the hadronic loops, while the solid curves are for adopting a dipole form factor.

tively) additions of the EM and hadronic loops with the dipole and monopole form factors are listed in comparison with the data.

In comparison with the results given by the on-shell approximation, it shows that the dispersive part of the loop transitions plays an important role in reproducing the data.

D. Hadronic loop contributions to the isospin violations in $J/\psi \to \omega\pi^0$

Similar to $\phi \to \omega\pi^0$, the decays of $J/\psi \to \omega\pi^0$ and $\psi' \to \omega\pi^0$ are also isospin-violating processes via the OZI doubly disconnected transitions. Their branching ratios are measured in experiment, i.e. $\mathrm{BR}(J/\psi \to \omega\pi^0) = (4.5 \pm 0.5) \times 10^{-4}$ and $\mathrm{BR}(\psi' \to \omega\pi^0) = (2.1 \pm 0.6) \times 10^{-5}$ [2], which are not significantly suppressed compared with $J/\psi(\psi') \to \phi\eta$, $\omega\eta'$, etc. An explanation based on vector meson dominance is provided in Refs. [11,12] where the branching ratios are fitted by EM transitions with an appropriate form factor. It also shows that process-I is the dominant contributions to the branching ratio while process-II is negligibly small. In this study, a natural question is about the role played by the hadronic loops and their contributions to the branching ratios.

Interestingly, $J/\psi \to K^*\bar{K}$ is one of the largest decay modes, from which relatively large couplings for the $J/\psi K^*\bar{K}$ vertex can be derived. However, due to the heavy mass of J/ψ, suppressions on the loop amplitudes become

TABLE II. The exclusive and coherent (constructive) contributions of the EM and hadronic loops to the $\phi \to \omega\pi^0$ branching ratios with a dipole and monopole form factor. The experimental data is the world average given by PDG2006 [2]. The branching ratios in columns 3–8 have a unit of 10^{-5}. The errors estimated in column 7 are due to the precisions taken for the exclusive branching ratios.

	Λ GeV	EM transition	$K\bar{K}(K^*)$	$K\bar{K}^*(K)$	$K\bar{K}^*(K^*)$	Total	Exp.
Dipole	2.14	1.66	0.23	0.33	~0.0	5.2 ± 0.2	$(5.2^{+1.3}_{-1.1})$
Monopole	1.38	1.66	0.14	0.56	~0.0	5.3 ± 0.5	$(5.2^{+1.3}_{-1.1})$

crucial. With the cancellation between the charged and neutral $K\bar{K}(K^*)$ loops, the hadronic loop contributions to the branching ratio turn out to be orders of magnitude smaller than the data. In ψ' decay, the cancellation between the charged and neutral $K\bar{K}^*(K)$ loops is not as significant as that in J/ψ where the branching ratios, $\text{BR}(J/\psi \to K^{*+}K^- + \text{c.c.}) = (5.0 \pm 0.4) \times 10^{-3}$ and $\text{BR}(J/\psi \to K\bar{K}^{*0} + \text{c.c.}) = (4.2 \pm 0.4) \times 10^{-3}$ are close to each other. In contrast, $\text{BR}(\psi' \to K^{*+}K^- + \text{c.c.}) = (1.7^{+0.8}_{-0.7}) \times 10^{-5}$ and $\text{BR}(\psi' \to K^{*0}\bar{K}^0 + \text{c.c.}) = (1.09 \pm 0.20) \times 10^{-4}$ have large differences, and have contained significant contributions from the EM transitions [11,12]. This favors maximizing the isospin violation effects in the hadronic loops. However, due to the suppression from the off-shell form factors, the hadronic loop contributions will still be negligibly small compared with the EM transitions.

The numerical calculations show that the branching ratios from the intermediate $K\bar{K}(K^*)$, $K\bar{K}^*(K)$, and $K\bar{K}^*(K^*)$ loops in $J/\psi(\psi') \to \omega\pi^0$ are orders of magnitude smaller than the data. This result suggests that the EM transition is likely the dominant isospin-violating process in the vector charmonium decays into light vector and pseudoscalar mesons. Thus, it enhances the argument [11,12] that the long-standing "$\rho\pi$ puzzle" in $J/\psi(\psi') \to$ VP is mainly due to the strong destructive interferences from the EM transitions in $\psi' \to \rho\pi$ which leads to the abnormally small branching ratio fraction of $\text{BR}(\psi' \to \rho\pi)/\text{BR}(J/\psi \to \rho\pi) \simeq 0.2\%$ [2].

IV. SUMMARY

We investigate the isospin-violating mechanisms in $\phi \to \omega\pi^0$ and $J/\psi \to \omega\pi^0$ by quantifying the EM and strong transitions as different sources of the isospin violations. The EM contribution is constrained in the VMD model, and the hadronic loop contributions is studied by relating them to the OZI-rule-violating processes. At hadronic level, the OZI rule violations are recognized through the nonvanishing cancellations between the charged and neutral intermediate-meson-exchange loops. In other words, the observation of the isospin-violating branching ratios can be viewed as a consequence of coherent contributions from the EM transitions and the nonvanishing cancellations among those intermediate meson exchanges due to the mass differences between the charged and neutral intermediate mesons and different couplings to the initial and final state mesons.

By extracting the vertex coupling information from independent processes, we can constrain the model parameters and make a quantitative assessment of the strong isospin violations via leading $K\bar{K}(K^*)$, $K\bar{K}^*(K)$, and $K\bar{K}^*(K^*)$ loops. It shows that the dispersive part of the hadronic loop amplitudes have important contributions to the isospin violation and they produce crucial interferences with the EM transitions though their exclusive contributions are relatively smaller than the EM ones in $\phi \to \omega\pi^0$ decay.

We also study the hadronic loop contributions to the isospin-violating decay of $J/\psi(\psi') \to \omega\pi^0$, and find that they are negligibly small. This is consistent with our previous study of the EM transitions in $J/\psi(\psi') \to$ VP, where we argued that the isospin-violating channels, such as $\omega\pi^0$, $\rho\eta$, $\rho\eta'$, and $\phi\pi^0$, were dominated by the EM transitions [11,12]. However, a caution should be given that in $J/\psi(\psi') \to$ VP the s dependence of the intermediate vector meson widths turns out to be a sensitive factor in account of contributions from light intermediate vector mesons. A coherent study of $e^+e^- \to \omega\pi^0$ over a broad range of s is thus strongly desired.

ACKNOWLEDGMENTS

G. Li would like to thank Y. L. Shen and W. Wang for useful discussions. This work is supported, in part, by the U.K. EPSRC (Grant No. GR/S99433/01), National Natural Science Foundation of China (Grants No. 10675131 and No. 10521003), and the Chinese Academy of Sciences (KJCX3-SYW-N2).

[1] M. N. Achasov *et al.*, Phys. Lett. B **449**, 122 (1999).
[2] W. M. Yao *et al.* (Particle Data Group), J. Phys. G **33**, 1 (2006).
[3] G. A. Miller, B. M. K. Nefkens, and I. Slaus, Phys. Rep. **194**, 1 (1990).
[4] A. Bramon, Phys. Rev. D **24**, 1994 (1981).
[5] J. F. Donoghue, B. R. Holstein, and D. Wyler, Phys. Rev. Lett. **69**, 3444 (1992).
[6] L. Ametller, C. Ayala, and A. Bramon, Phys. Rev. D **30**, 674 (1984).
[7] S. A. Coon, B. H. J. McKellar, and M. D. Scadron, Phys. Rev. D **34**, 2784 (1986).
[8] S. A. Coon and R. C. Barrett, Phys. Rev. C **36**, 2189 (1987).
[9] H. Genz and S. Tatur, Phys. Rev. D **50**, 3263 (1994).
[10] N. N. Achasov and A. A. Kozhevnikov, Int. J. Mod. Phys. A **7**, 4825 (1992).
[11] Q. Zhao, G. Li, and C. H. Chang, Phys. Lett. B **645**, 173 (2007).
[12] G. Li, Q. Zhao, and C. H. Chang, arXiv:hep-ph/0701020.
[13] A. Aloisio *et al.* (KLOE Collaboration), Phys. Lett. B **561**, 55 (2003); **609**, 449(E) (2005); arXiv:hep-ex/0303016.
[14] H. J. Lipkin, Nucl. Phys. **B291**, 720 (1987).
[15] H. J. Lipkin, Phys. Lett. B **179**, 278 (1986).
[16] P. Geiger and N. Isgur, Phys. Rev. D **47**, 5050 (1993).
[17] N. Isgur and H. B. Thacker, Phys. Rev. D **64**, 094507

(2001).
[18] H. J. Lipkin and B. S. Zou, Phys. Rev. D **53**, 6693 (1996).
[19] J. J. Wu, Q. Zhao, and B. S. Zou, Phys. Rev. D **75**, 114012 (2007).
[20] Y. Lu, B. S. Zou, and M. P. Locher, Z. Phys. A **345**, 207 (1993).
[21] X. Q. Li, D. V. Bugg, and B. S. Zou, Phys. Rev. D **55**, 1421 (1997).
[22] Q. Zhao, B. S. Zou, and Z. B. Ma, Phys. Lett. B **631**, 22 (2005).
[23] Q. Zhao, Phys. Lett. B **636**, 197 (2006).
[24] X. Liu, X. Q. Zeng, and X. Q. Li, Phys. Rev. D **74**, 074003 (2006).
[25] T. Bauer and D. R. Yennie, Phys. Lett. **60B**, 169 (1976).
[26] N. A. Tornqvist, Ann. Phys. (N.Y.) **123**, 1 (1979).
[27] Q. Zhao and B. S. Zou, Phys. Rev. D **74**, 114025 (2006).